EMPIRICAL ORTHOGONAL FUNCTION ANALYSIS OF MAGNETIC OBSERVATORY DATA: FURTHER EVIDENCE FOR NON-AXISYMMETRIC MAGNETOSPHERIC SOURCES FOR SATELLITE INDUCTION STUDIES

Georgios Balasis[(1)], Gary D. Egbert[(2)]

[(1)]GeoForschungsZentrum Potsdam, Telegrafenberg, D-14473 Potsdam, Germany, Email: gbalasis@gfz-potsdam.de
[(2)] College of Oceanic and Atmospheric Sciences, Oregon State University, Oceanography Admin. Bldg. 104, Corvallis, OR 97331-5503, USA, Email: egbert@coas.oregonstate.edu

ABSTRACT/RESUME

Although satellite electromagnetic induction studies have usually assumed a symmetric magnetospheric ring current source, there is growing evidence for significant source asymmetry. Here we apply empirical orthogonal function methods to mid-latitude night-side hourly mean geomagnetic observatory data to search for evidence of non-zonal low-frequency source fields. The dominant spatial mode of variability in residuals, obtained by subtracting symmetric ring current and ionospheric fields of the CM4 comprehensive model, has a substantial Y_2^{-1} quadrupole component and is highly correlated with D_{st}. This pattern of temporal variability, which implies enhanced ring current densities in the dusk sector, persists even when peak storm-time data are omitted. The observed asymmetry agrees with that inferred previously [1], from the local time dependence of biases in satellite induction transfer functions. Temporal correlation of the leading mode with D_{st}, and consistency of its spatial structure with recent empirical ring current models, suggest a magnetospheric origin.

1. INTRODUCTION

The traditional approach to estimation of the electrical conductivity of Earth's mantle is based on interpretation of ground-based observatory recordings of geomagnetic variations of external origin on time scales from hours to months [2 – 5]. This approach has a serious inherent limitation: the global distribution of magnetic observatories is irregular and sparse, leaving large areas of the Earth (especially the ocean basins) unsampled. Recent magnetic satellite missions, such as Oersted, CHAMP, and SAC-C provide nearly complete global coverage, and thus offer exciting possibilities for new insight into 3D patterns of mantle conductivity. However, to date electromagnetic (EM) induction studies with satellite data [6 – 10] have all been based on very simple models of the external sources: a symmetric magnetospheric ring current (RC) described by Y_1^0, and possibly a few other zonal harmonics.

Reference [1] (hereinafter BEM) show that estimates of EM induction transfer functions (TFs) obtained from CHAMP data under the traditional assumption of a symmetric RC source have biases which depend systematically on local time (LT). This pattern of biases suggests that a purely zonal source model is inadequate. BEM further showed that the pattern could be explained by adding a Y_2^1 quadrupole term correlated with the traditional axial dipole source variations, and oriented so that meridional magnetic fields peak in the dusk sector (at 19:30 LT).

There has long been evidence for asymmetry in the RC, particularly for the storm main phase [11 – 12]. But are these asymmetries only brief, lasting for a few hours near storm onset? Or are they persistent enough that they must be accounted even for very long period induction studies, as the results of BEM suggest? Only recently has clear evidence been presented for asymmetry of the RC at all activity levels [13 – 14]. These two studies used in situ satellite data to directly map long term average magnetospheric current densities as a function of D_{st}. Systematic differences of average current densities between activity levels, and persistence of asymmetries (with the strongest fields centered in the midnight and dusk sectors) suggest long period variations of the asymmetric RC, closely coupled to activity level and D_{st}, consistent with the indirect inference of asymmetry by BEM.

Here we use geomagnetic observatory data to investigate this issue further, applying a novel analysis to emphasize signals which vary slowly in a solar magnetic (SM) reference frame. A major advantage of this data set is that each observatory sweeps through all LTs once per day, providing direct observation of non-zonal structure. A disadvantage is that ground-based observations by themselves cannot distinguish magnetospheric and ionospheric sources, and ionosphere currents exhibit very strong LT dependence. We take two steps to minimize ionospheric complications: (1) we subtract the CM4 comprehensive model [15] ionospheric correction; and (2) we focus on night-side mid-latitude data where ionospheric contamination is expected to be least.

2. DATA PROCESSING

We analyzed three component hourly mean geomagnetic data, starting with 79 observatories at all latitudes, for 4 years (1997 – 2000).

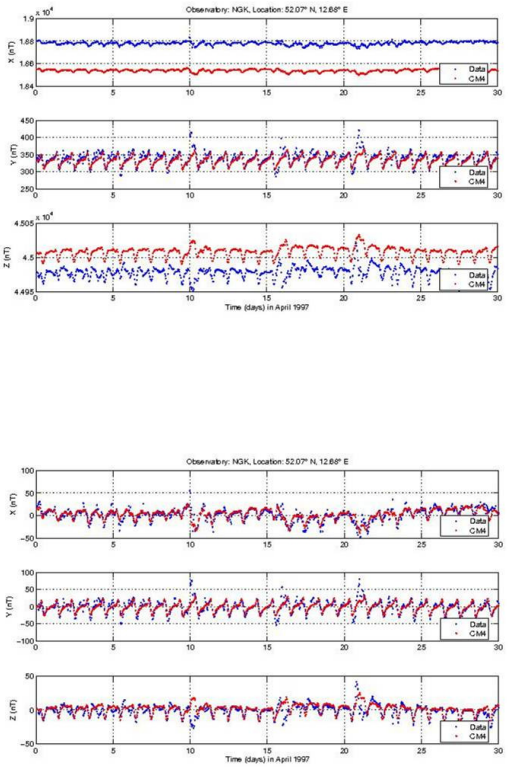

Figure 1. Geomagnetic time series in Niemegk observatory for November 1997 and CM4 prediction for the same time interval: without (upper panel) and with (lower panel) correction for the baseline shift.

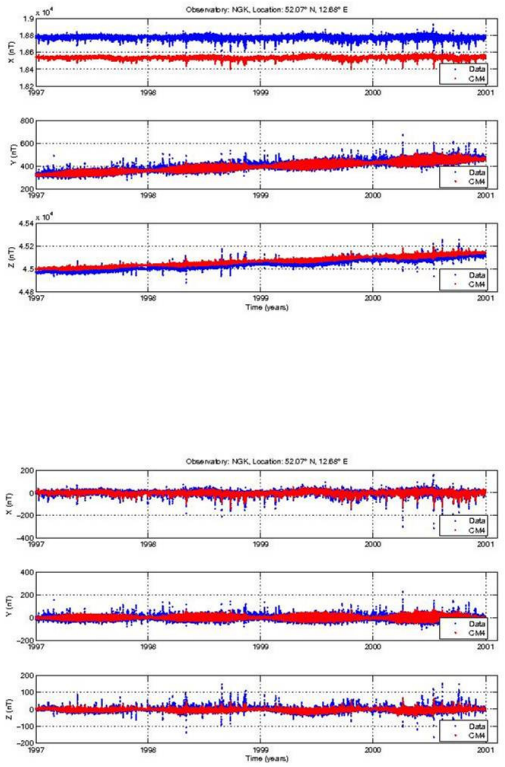

Figure 2. Geomagnetic time series in Niemegk observatory from 1997 to 2000 and CM4 predictions for the same time interval: without (upper panel) and with (lower panel) correction for the baseline shift.

The following preliminary processing steps were then applied:

1) The CM4 model with the E-region ionospheric orrection driven by the daily $F_{10.7}$ solar flux index, and with symmetric RC variations driven by D_{st}, was subtracted. This removes much (but certainly not all) of the regular daily variation of ionospheric origin, approximately accounting for modulation in the size of the ionospheric cavity [15]. The D_{st} dependent part of CM4 correction also removes most of the axisymmetric RC variation and corresponding induced fields. After correction with the CM4 (Fig. 1 – 2), residual observatory means were subtracted (to remove short wavelength crustal fields not represented in the CM4), and each channel was high-pass filtered with a 50 day cut-off.

2) Time series for each observatory were interpolated from the standard hourly sampling at fixed UT, to fixed hourly sampling in magnetic local time (MLT). Daily sections of the filtered residual magnetic fields were then constructed with the data for all observatories aligned by MLT, and sorted by geomagnetic latitude (Fig. 3). For the 4 year period this results in 1439 one day sections each with 79 x 24 "pixels", each corresponding to one observatory at a fixed MLT. With this alignment, low frequency (f << 1 cycle per day) external source variations in a SM frame are sampled at all longitudes (and at the geomagnetic latitudes of the observatories) once per day.

3) Time series for each pixel were low-pass filtered with a 5 day cut-off. This filtering reduces the effects of more rapid variations which might be more appropriately described in UT, but does not smooth non-axisymmetric spatial structure in the SM frame. As illustrated in Fig. 3, the combined effect of this filtering and alignment of the data by MLT produces smoother and cleaner looking daily samples of the

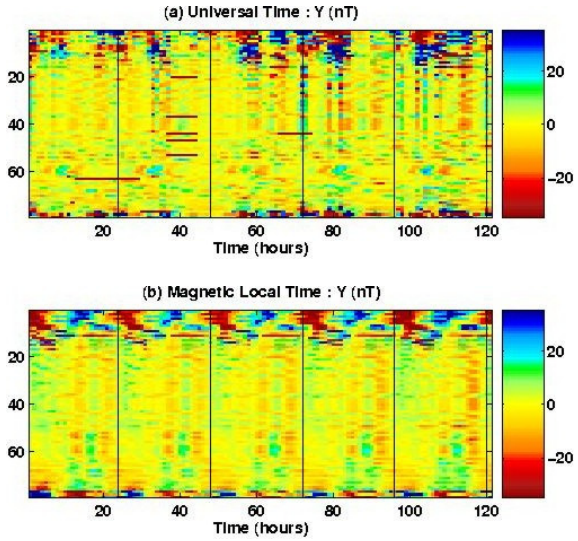

Figure 3. Example of residuals (geomagnetic east component) for 5 days of data from 79 observatories, after subtraction of CM4 predictions, before (a) and after (b) aligning and smoothing as described in text. The data are sorted by geomagnetic latitude N to S (axis on left is observatory number with geomagnetic dipole equator near number 65). Vertical lines denote day boundaries; each 79 x 24 panel is one (spatial) realization for the EOF decomposition.

magnetic fields.

4) Seasonal means, averaging over all days in the winter (Nov – Feb), summer (May – Aug) and equinox months were subtracted. These means are strongly dominated by auroral current systems (which CM4 does not explicitly model) but there are also spatially coherent corrections of the order of 5 nT at mid-latitudes.

Special care was taken for missing data in steps 1 – 4: they were excluded from computation of means, set to 0 after subtracting means, and omitted from the calculation of averages when pixels were low-pass filtered. After these initial processing steps, we applied an empirical orthogonal function analysis (EOF, also known as principal component analysis; e.g., see [16]) to the time sequence of residual daily magnetic field vector variations. The EOFs decompose the total time varying signal into a sum over spatio-temporal modes: $H\ (\vartheta,\ \varphi,\ t) = \sum_k X_k\ (\vartheta,\ \varphi)\ T_k\ (t)$. Note that here ϑ represents observatory (geomagnetic) latitude, and φ MLT. The leading spatial mode $X_1\ (\vartheta,\ \varphi)$ is the pattern of three component magnetic field vectors that explains the most variance in the sequence of daily sections. The corresponding temporal function $T_1\ (t)$ gives the time varying coefficient (or loading) of the spatial mode. Additional modes are orthogonal in space, and in time (i.e., the temporal modes are uncorrelated), and

Table 1. Spherical harmonic model fitted to first EOF.

Degree	Order	Coefficient	Error
1	0	0.0244	.0005
2	-1	-0.0218	.0004
4	-1	-0.0031	.0002
5	-1	0.0014	.0002
5	0	0.0016	.0002

explain successively less of the residual variance. The EOF decomposition is essentially just the singular value decomposition (SVD) of the full data matrix, where rows of the data matrix represent spatial position (both latitude and longitude), and the columns represent replicates over time. The singular values give the relative amplitudes of each data mode. For the observatory analysis described here roughly 50 % of the residual variance is contained in the first 3 – 4 modes with roughly 20 % in the first mode alone, depending on details of the pre-processing.

3. RESULTS

The leading EOF modes obtained from analyzing observatories from all latitudes and all MLTs are dominated by auroral current systems, but there are significant large scale corrections at mid-latitudes as well. To focus on the asymmetries in magnetospheric sources suggested by the BEM results, which were based on mid-latitude night-side satellite data, we restricted the EOF analysis to observatories between 50°S and 50°N geomagnetic, and to MLTs for the 12 hour period centered on local midnight. The first mode (Fig. 4) indeed shows clear evidence for the large scale non-axisymmetric signal inferred by BEM. Note that the temporal variation of this signal is very clearly correlated with D_{st} (Fig. 4a). The positive correlation of $T_1\ (t)$ with D_{st} means that fluctuations in magnetic fields on the Earth surface associated with the storm time variations tracked by D_{st} exhibit persistent asymmetries, with peak amplitudes centered in the dusk sector. In Fig. 4 $T_1\ (t)$ is scaled to be comparable to D_{st}, so the scale of the spatial mode gives the relative amplitude, normalized to the symmetric RC component, of the asymmetry. The first EOF thus corresponds to variations in the north component (X) that are of the order of 10 – 15 % of the symmetric D_{st} component. The other leading EOFs (only the first and second are shown here) also exhibit large scale spatial structure but are increasingly noisy. These EOFs also reveal evidence for seasonal variations, suggesting that the treatment of seasonal effects in CM4 could be further refined [see also 17]. When storm commencement data are excluded prior to step 3 (e.g., omitting all data with $D_{st} < -75$ nT) very similar results are obtained for the EOF analysis.

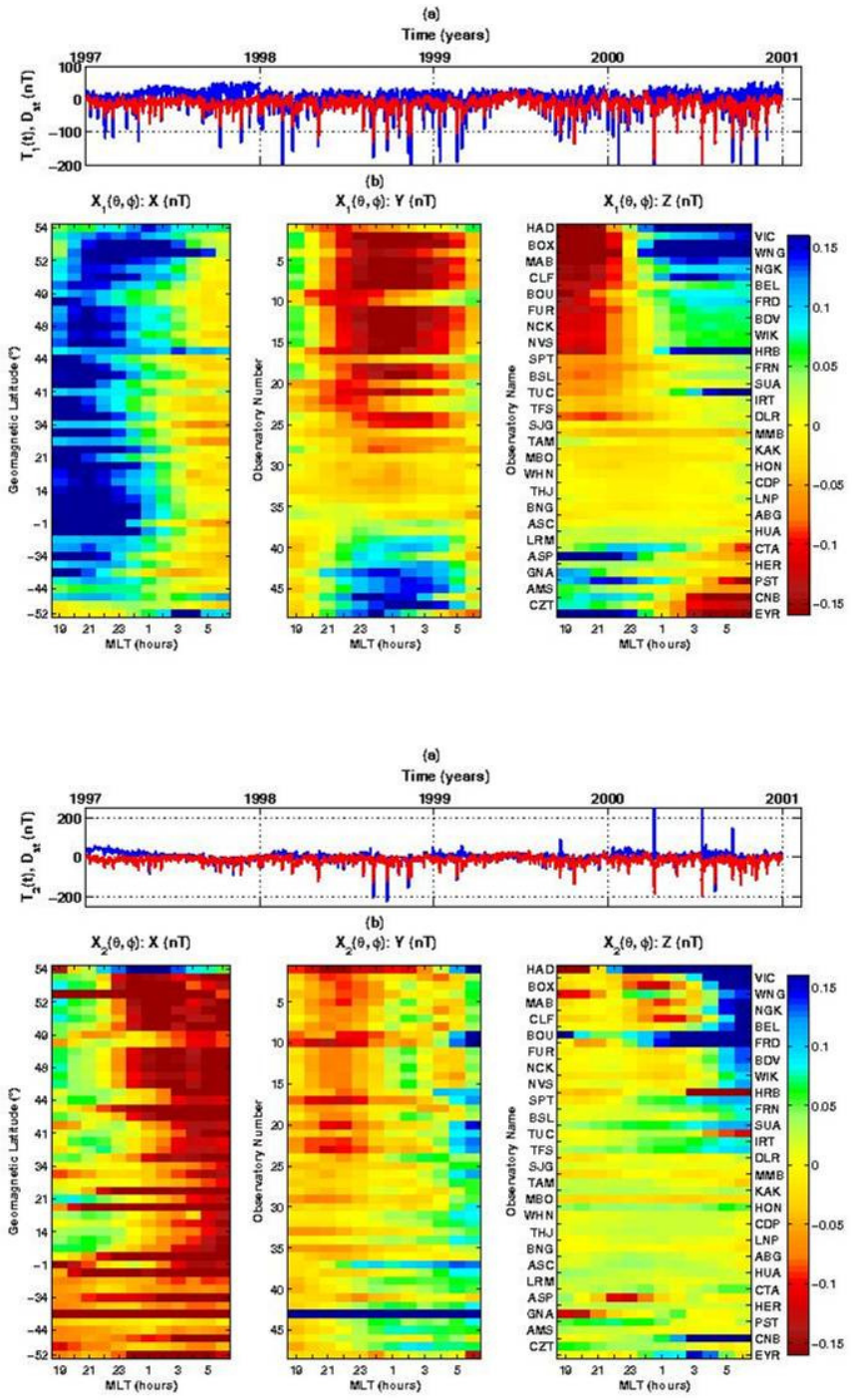

Figure 4. First (upper panel) and second (lower panel) EOF of the mid-latitude night-side magnetic observatory data, after processing outlined in text. (a) EOF time variation T_1 (t) (blue curve) scaled to be comparable to D_{st} (red curve). (b) three components of the spatial mode X_1 (ϑ, φ), in geomagnetic coordinates. Geomagnetic latitude, observatory number, and code are given on the y axes of the X, Y and Z plots, respectively.

We used least squares to fit the horizontal components of the leading spatial mode (12 x 48 x 2 = 1152 elements) as the gradient of a scalar potential expanded in spherical harmonics to degree and order 5 (35 parameters). A backwards elimination procedure, using a 0.99 significance level [18], was used to eliminate spherical harmonics which did not contribute significantly to the fit. The resulting model, given in Tab. 1, includes 5 terms and fits the EOF with R^2 = 0.82, nearly as well as the full degree 5 expansion (R^2 = 0.85). Three terms dominate: together Y_2^{-1}, Y_1^0, and Y_4^{-1} explain most of the variance (R^2 = 0.79).

4. DISCUSSION

Empirical orthogonal function analysis of night-side (18:00 – 06:00 MLT) mid-latitude (50°S to 50°N) observatory data show clear evidence for large scale non-axisymmetric structure that is fixed in MLT, coherent with D_{st}, and persists even when storm commencement data are excluded. The significant Y_2^{-1} quadrupole component in the first mode EOF magnetic fields implies an enhancement of RC density in the dusk sector, and meridional current on the night-side centered near local midnight. Examination of Fig. 4 suggests that the peak in RC density is in fact shifted several hours towards local midnight, consistent with the alignment of the asymmetry inferred by BEM. The pattern in the dominant EOF is also in broad agreement with the recent empirical RC models of Jorgensen et al. [13] and Le et al. [14], which exhibit persistent peaks in outer RC density in the dusk and midnight sectors. In particular Le et al. found that on average the peak of the RC shifts towards the dusk sector for higher D_{st} levels. This is consistent with the strong positive correlation between D_{st} and the dominant EOF from our analysis. The spatial structure of the dominant EOF also agrees well with the Tsyganenko model [19] for the partial RC.

We cannot completely rule out the possibility that the asymmetry observed in the observatory data has an ionospheric origin. However, in addition to the agreement between our results and the empirical maps of magnetospheric RC densities, two further lines of evidence support a magnetospheric source for the observed asymmetries. Most striking is the very strong correlation of the temporal loading of the dominant EOF with D_{st} (Fig. 4a). This strong correlation would be very surprising if the asymmetry were not due dominantly to magnetospheric sources [11]. Second, BEM indirectly inferred the same pattern of magnetospheric RC asymmetry from the LT dependence of induction TF biases estimated from CHAMP satellite magnetic data. Since CHAMP flies above the ionosphere and below the magnetosphere, the satellite data can distinguish between ionospheric and magnetospheric sources. BEM found that the observed pattern of biases could be readily explained by addition of a quadrupolar source peaked near dusk (i.e., essentially Y_2^{-1}) that was external to the satellite orbit (i.e., magnetospheric), but not by similar internal (i.e., ionospheric) non-axisymmetric sources.

Because of Earth rotation any slowly varying non-axisymmetric structure will in fact result in induction at daily variation periods; only the axisymmetric part of the RC will contribute to induction at long periods. However, accurate models of the non-axisymmetric signal will still be essential to proper interpretation of the satellite data, since these components will appear in the satellite frame as slowly varying components of the magnetic field. Given the growing body of evidence for asymmetry in the RC, we suggest that further progress in satellite induction studies will require moving beyond the simple axisymmetric source field models used to date. Proper interpretation of the satellite data will also require accurate separation of ionospheric and magnetospheric sources, as these will be respectively internal and external to the satellite orbit. Interconnections between magnetospheric and ionospheric current systems will also have to be modeled properly. For example, the meridional currents associated with the dominant EOF of Fig. 4 almost certainly flow along field lines, and close in the auroral ionosphere. Thus, these currents will be partly external, and partly internal, to the satellite orbit.

Combination of both satellite and observatory data will be essential to the task of developing improved source models for induction studies. Our study here using only observatory data, combined with the study of BEM using only satellite data provides a glimpse of the potential power of combining these multiple data sources. The asymmetry is well mapped by the observatories in this study; incorporating the CHAMP results from BEM implies that the asymmetry most likely comes from the magnetosphere. Future work should combine these two data sources more explicitly to further improve separation and characterization of ionospheric and magnetospheric sources. Obviously we also need to take advantage of the existing extensive observational, theoretical, and modeling studies of the magnetosphere to guide development of the more realistic models for magnetospheric (and ionospheric) sources that will be required for progress in satellite induction studies. Statistical estimates of average magnetospheric RC densities and/or semi-empirical models such as that of Tsyganenko [19] might be useful starting points for these developments. Ultimately, data assimilation methods which combine physics-based models of the magnetosphere and ionosphere with all available data offer the greatest hope for accurate modeling of external sources for global induction studies with satellite data.

5. REFERENCES

1. Balasis G., Egbert G. D. and Maus S., *Geophys. Res. Lett.*, Vol. 31, doi:10.1029/2004GL020147, 2004.

2. Banks R. J., *Geophys. J. R. astr. Soc.*, Vol. 17, 457 – 487, 1969.
3. Schultz A. and Larsen J. C., *Geophys. J. Int.*, Vol. 101, 565 – 580, 1990.
4. Olsen N., *Geophys. J. Int.*, Vol. 133, 298 – 308, 1998.
5. Fujii I. and Schultz A., *Geophys. J. Int.*, Vol. 151, 689 – 709, 2002.
6. Olsen N., *Surv. in Geophys.*, Vol. 20, 309 – 340, 1999.
7. Tarits P. and Grammatica N., *Geophys. Res. Lett.*, Vol. 27, 4009 – 4012, 2000.
8. Martinec Z. and McCreadie H., *Geophys. J. Int.*, Vol. 157, 1045 – 1060, 2004.
9. Velimsky J., Martinec Z. and Everett M. E., *Geophys. J. Int.*, in press, 2006.
10. Constable S. and Constable C., G^3, doi:10.1029/2003GC000634, 2004.
11. Daglis I. A. and Kozyra J. U., *J. Atmos. Solar-Terr. Phys.*, Vol. 64, 253 – 264, 2002.
12. Daglis I. A. et al., *J. Geophys. Res.*, Vol. 108, doi:10.1029/2002JA009722, 2003.
13. Jorgensen A. M. et al., *J. Geophys. Res.*, Vol. 109, doi:10.1029/2003JA010090, 2004.
14. Le G., Russell C. T. and Takahashi K., *Annales Geophysicae*, Vol. 22, 1267 – 1295, 2004.
15. Sabaka T. J., Olsen N. and Purucker M. E., *Geophys. J. Int.*, Vol. 159, 521–547, 2004.
16. Preisendorfer R. W., *Principal Component Analysis in Meteorology and Oceanography*, Elsevier, Amsterdam, 1988.
17. Maus S. and Lühr H., *Geophys. J. Int.*, Vol. 162, 55 – 763, 2005.
18. Kleinbaum D. G. and Kupper L. L., *Applied regression analysis and other multivariable methods*, Duxbury, Boston, 1978.
19. Tsyganenko N. A., *J. Geophys. Res.*, Vol. 107, doi:10.1029/2001JA000220, 2002.